Electrochemical Analysis of the Corrosion Kinetic of Carbon Steel in LiBr Solution

A. Soliz* and L. Cáceres

CICITEM, Centro de Investigación Científico y Tecnológico para la Minería, Departamento de Ingeniería Química y Procesos de Minerales, Facultad de Ingeniería, Universidad de Antofagasta, Av. Angamos 601, Antofagasta, Chile.
*Corresponding author: Tel.: +56 55 2637313; E-mail address: alvaro.soliz@uantof.cl (A. Soliz)

ABSTRACT

The effect of exposure time to the corrosion kinetic behavior of carbon steel type AISI 1020 was studied using potentiodynamic polarization technique in an aerated 0.5 mol/L LiBr solution. From experimental polarization curves, the kinetics of partial corrosion reactions was analyzed using the superposition model in terms of mixed potential theory. Noticeable changes, mainly on the kinetics parameters for the oxygen reduction reaction, were related to the corrosion products deposited on steel surface, retarding the mass transfer of dissolved oxygen from the bulk solution to metallic surface. Under this circumstances where the corrosion rate is highly dependent with the oxygen concentration, it was found that the corrosion rate have different tendencies with the exposure time, which increase during the first immersion hours and gradually decrease at long exposure times. Changes on the control mechanism of corrosion process also were discussed.

Keywords: Carbon steel; Polarization curve; Kinetic parameters

1. INTRODUCTION

A range of standard techniques is available to study electrochemical behavior of conductive and semi-conductive materials [1, 2]. The requirements to use these techniques are extensively described in reference literature [3, 1]. However, the applications of some techniques to rapid reactions are often complicated by need to make relatively large corrections [4]. Typically, the estimation of kinetic parameters is performed by using the Tafel extrapolation method, which requires that both anodic and cathodic reactions presents a charge transfer control and well-defined branches over at last one decade of current [5]. In this sense, various electrochemical processes do not display an extensive linearity in Tafel region, and the applicability of this technique could cause future erroneous readings.

Several researches have investigated the iron and steel corrosion process under a large variety of conditions, mostly on cylindrical and planar surfaces. In all cases, the mass transfer rate of species play an important role in the determination of the corrosion rate. Particularly, behavior that involves the dissolution mechanism of iron and its dependence on the hydrodynamic and the dissolved oxygen concentration [6, 7], in where the influence of different oxide phases that precipitate as corrosion products causes changes on the kinetic behavior of partial corrosion reactions. In many cases, the corrosion process occurs under the condition of mixed kinetics. Under aerated and near neutral solutions, the activity of hydrogen protons is too low to participate in the hydrogen evolution reaction, and under this circumstances the water molecules acts as the electron acceptor [7]. On the other hand, under aerated conditions of the electrolytic solution, the oxygen reduction becomes to be the main reaction, which principally proceeds by a mixed charge-transfer and diffusion control mechanism [8-10].

In this work the influence of the exposure time on the kinetic corrosion parameters of carbon steel immersed in diluted LiBr solution was studied from the synthesis of experimental polarization curves by using the superposition model.

2. EXPERIMENTAL

Electrochemical measurements were performed in a conventional three-electrode glass cell with a rotating disk electrode (RDE) system. The working electrodes were made from small cylindrical carbon steel type AISI 1020 bars that has a chemical composition of (wt%): 0.2 C, 0.6 Mn, 98.5 Fe and traces of S, Si, Cu, Ni, Cr, Sn, P and Mo. The specimen with a cylindrical shape (4 mm diameter and 10 mm of length) were inserted into a plastic rod (8 mm diameter and 20 mm of length) and sealed applying resin adhesive, so that only the bottom planar surface (area 1.26×10^{-5} m^2) was exposed to the test solution. A saturated Ag/AgCl electrode and a platinum spiral wire served as reference and auxiliary electrodes, respectively. The test solution (0.5 mol/L LiBr) was prepared at room temperature using analytical grade reagents and distilled water. Before the experiments, the working electrodes were polished with SiC sand paper from 600 to 1200 grit, degreased with ethanol in a ultrasonic bath, and cleaned with distilled water. On the other hand, high purity air gas was bubbled into the solution during 30 min and was maintained till the end of the experiences, in order to maintain a constant oxygen concentration.

Current density-potential polarization curves were recorded as function of the immersion time at 2500 rpm and a scan rate of 1 mV/s using an EPSILON potentiostat/galvanostat (Bas Inc. USA) model BAS100 B/W provided with a rotating electrode interface BAS/RDE-1. All potentials reported in this work were referred at the Standard Hydrogen Electrode (SHE).

3. RESULTS AND DISSCUSION

a. Electrochemical measurements

Figure 1 shows potentiodynamic polarization curves obtained for carbon steel electrodes immersed in aerated unbuffered 0.5 mol/L

LiBr solution at different exposure times. On the cathodic branch, it is seen that the current density values decrease with decreasing the cathode potential at potentials more negatives than -750 mV/SHE, followed by the presence of a planar plateau at potentials between -750 and -450 mV/SHE, and finally converge to zero total current density at the corrosion potential (E_{corr}). These variations on the cathodic region primarily are attributed to hydrogen evolution reaction (HER) and oxygen reduction reaction (ORR), which can be represented by a charge transfer control and a mixed mass transfer and charge transfer control mechanism, respectively. On the other hand, the current inversion observed at potentials more positives than that E_{corr} correspond to iron oxidation in where the anodic current density increases without the presence of a passive layer.
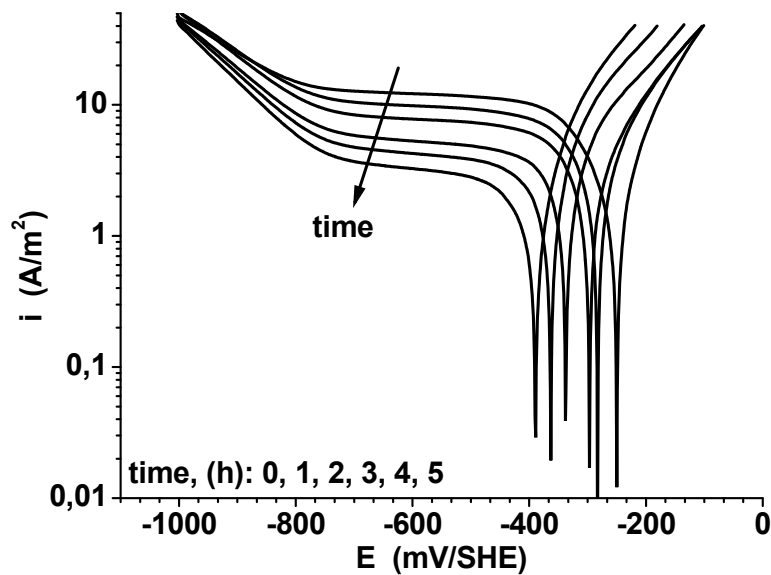

Figure 1. Experimental polarization curves for carbon steel electrodes in 0.5 mol/L LiBr, at different exposure time

As can be seen from the Figure 1, all polarization curves presents similar shapes at different immersion times. In the figure, it is seen that the current density of the planar section, corresponding to the mass transfer control mechanism, decreases continuously with the exposure time associated at a reduction on its overpotential range. These variations are attributed to formation and growth of a passive layer on the metallic surface, causing a decrease in the mass transport of dissolved oxygen from the bulk solution to metallic surface [6]. In addition to this, it can be recognized that the potential of the current density inversion shifts to more negative potentials as the exposure of the electrodes in the aggressive solution is increasing. This shift of corrosion potential typically is caused by the presence of an anaerobic behavior near to the solid-liquid interface [11, 6]. Furthermore, a particular observation on the anodic branch is the absence of a planar plateau due to the formation of a passive layer. It can be related to the formation of a porous structure for the passive layer [12, 13], allowing a continuous dissolution of the steel. Many works mentioned that under a limited oxygen supply, the oxide phase of magnetite (Fe_3O_4) is more likely to form [14, 15], in contrast with an enough oxygen supply, in where lepidocrocite (-FeOOH), maghemite (-Fe_2O_3) and hematite (-Fe_2O_3) are principally formed [6, 13].

b.   Kinetic and corrosion parameters

As alternative to use the Tafel extrapolation method to determinate kinetic and corrosion parameters, the superposition model in terms of the mixed potential theory was used in this work to analyze the corrosion kinetic from

$$i = i_{O2} + i_{H2} + i_{Fe} \tag{1}$$

where, i_{O2}, i_{H2}, and i_{Fe} are the partial current densities of the ORR, HER, and iron oxidation, respectively.

experimental polarization curves [7, 11], in where the total current density i can be expressed by:

This model considers a charge transfer control of the HER and iron oxidation, and a mixed control mechanism of ORR [9-11], in where the Eq. (1) becomes:

$$i_{O2} = (i_{(0,O2)} \exp(2.303(E - [Eq]_{O2})/b_{O2}))/(1 + [(i)_{(0,O2)}/[(i)_{(l,O2)}]\exp(2.303(E - [Eq]_{O2})/b_{O2})) \tag{2}$$

$$i_{H2} = i_{0,H2} \exp\left(\frac{2.303(E - E eq_{H2})}{b_{H2}}\right) \tag{3}$$

$$i_{Fe} = i_{0,Fe} \exp\left(\frac{2.303(E - Eq_{Fe})}{b_{Fe}}\right) \tag{4}$$

where, i_0, b, and E_{eq} are the exchange current density, Tafel slope, and the equilibrium potential with subscripts of oxygen reduction, hydrogen evolution and iron oxidation respectively, E is the applied potential and $i_{l,O2}$ is the limiting current density for oxygen reduction.

The kinetic and corrosion parameters were determined according to the methodology previously published based on the minimization of the total sum of the squared values [7, 11].

Figure 2 shows the experimental and fitted polarization curves, in addition to the partial polarization curves that were synthetized using kinetic parameters listed in Table 1.

The fitted data is in agreement with those experimental data, validating the applicability of the mixed potential theory in corrosion studies. In the figure, the corrosion potential (E_{corr}) and corrosion current density (i_{corr}) were obtained under a zero total current density condition (i = 0 A/m^2).
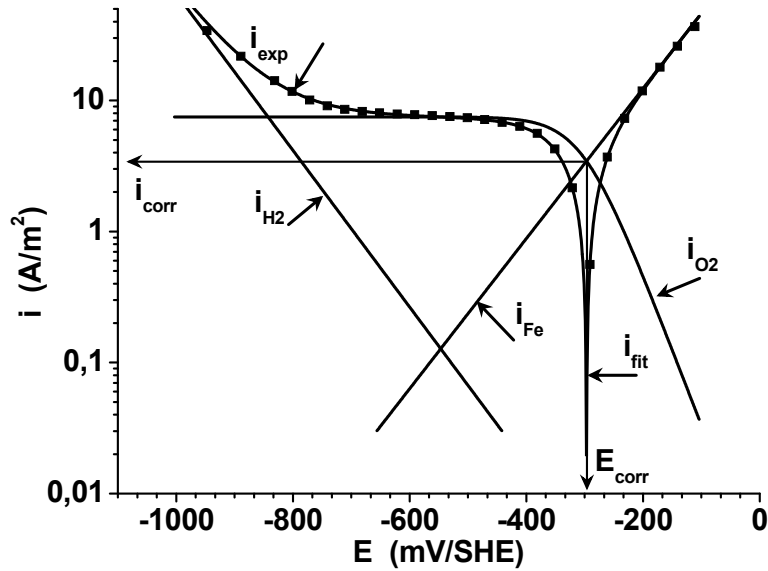
Figure 2. Experimental, fitted and partial polarization curves for carbon steel in 0.5 mol/L LiBr solution at 2500 rpm.

In Table 1, it was observed that the anodic Tafel slopes for a oxide-free surface was 127 mV/dec, however it was increasing to 181 mV/dec followed by a decrease to 138 mV/dec for longer exposure times. It fluctuations mainly are caused by changes on the state of surface by forming a protective layer. On the other hand, it was observed that the hydrogen Tafel slope no presents high variations suggesting no appreciable influence of the exposure time. In contrast with iron and hydrogen Tafel slope values, the oxygen Tafel slope were decreasing continuously with the exposure time up to reach constant values at longer times. These changes in $|b_{O2}|$ can be explained in term of the surface coverage and the nature of the passive film deposited on the metallic surface [16]. The difference between $|b_{O2}|$ values from an oxide-free surface, clearly indicates a reduction of the available active sites for the oxygen adsorption and their further O-O bond breakdown, due to the high coverage surface by different oxide phases. This tendency also is confirmed by decreases on exchange current density values, which are related directly to the equilibrium behavior.

Table 1. Kinetic and corrosion parameters for carbon steel in aerated 0.5 mol/L LiBr at different exposure time

Time, (h)	Iron oxidation		Hydrogen evolution		Oxygen reduction			
	b_{Fe}, (mV/dec)	$i_{0,Fe}$, (A/m^2)	b_{H2}, (mV/dec)	$i_{0,H2}$, (A/m^2)	b_{O2}, (mV/dec)	$i_{0,O2}$, (A/m^2)	$|i_{l,O2}|$, (A/m^2)	E_{corr}, (mV/SHE)
0	127	4.13×10^{-3}	-160	-0.023	-116	-7.50×10^{-9}	11.95	-252
1	181	6.27×10^{-2}	-164	-0.033	-107	-1.31×10^{-9}	9.61	-282
2	175	5.13×10^{-2}	-167	-0.037	-86	-3.37×10^{-12}	7.50	-297
3	175	8.82×10^{-2}	-159	-0.024	-48	-1.13×10^{-22}	5.18	-337
4	145	5.83×10^{-2}	-168	-0.031	-41	-7.45×10^{-27}	4.05	-362
5	138	6.77×10^{-2}	-163	-0.023	-34	-1.71×10^{-32}	3.13	-389
Av.	157	5.54×10^{-2}	-164	-0.028	-72	-1.47×10^{-9}	6.90	-320

It exposure time dependency observed on the ORR also affect the limiting current density ($i_{l,O2}$), E_{corr} and i_{corr} values. To visualize this influence, values of $i_{l,O2}$ and i_{corr} were plotted in Figure 3. In this figure, the $i_{l,O2}$ values were decreasing continuously with the exposure time, confirming a lower mass transport rate of dissolved oxygen to the metallic surface. On the other hand, the i_{corr} values were increasing during the first hour of immersion, followed by a decrease at longer exposure times. It results are according with the anodic and cathodic Tafel slopes fluctuations. According to these results, it can be indicate that the iron dissolution process at the solid-liquid interface occurs simultaneously with the oxide growth at the metal-oxide interface, which restrict the flux of oxidative species.

Furthermore, due to variations on dissolved oxygen concentration at solid-liquid and solid-oxide interface, the degree of incidence of oxygen mass transport on corrosion kinetic behavior can be visualized through the $i_{l,O2}/i_{corr}$ relationship as is depicted in the inset of Figure 3. In the figure, a significant increase of the degree of incidence was observed at longer exposure times, indicating a change on the ORR kinetic, which going of a mixed control to a pure diffusion control mechanism. Under this behavior, the limiting current density begin equal to corrosion current density.
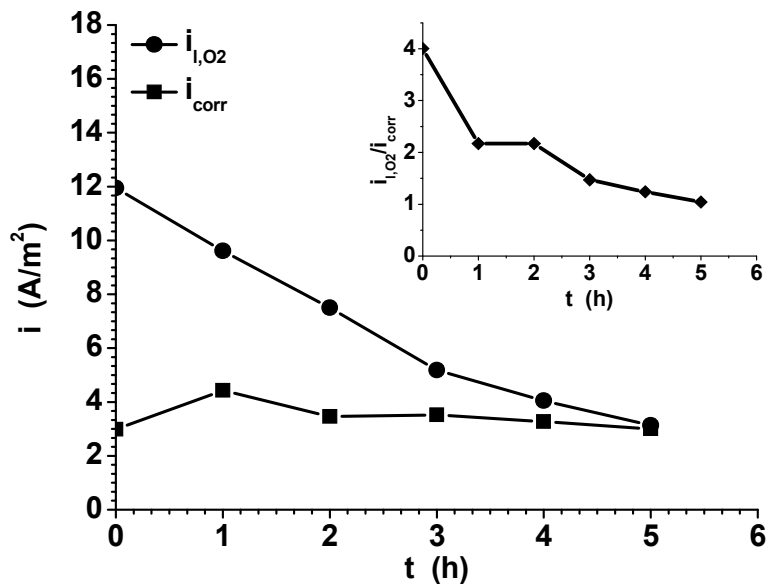

Figure 3. Dependence of corrosion current density and limiting current density for the ORR on the exposure times for carbon steel electrodes in 0.5 mol/L LiBr solution. Inset figure shows the degree of mass transfer incidence.

4. CONCLUSIONS

Important information concerning the corrosion kinetic for carbon steel in 0.5 mol/L LiBr solution have been considered by applying non-linear fitting using the superposition model. The comparison between kinetics parameters for partial corrosion reactions indicates that the oxygen reduction reaction exhibited a high dependence with the exposure time, in contrast with the kinetic behavior for iron oxidation and hydrogen evolution reaction. It dependence leads to changes on the mechanism control for the oxygen reduction, from a mixed control to a pure mass transfer control. Additionally, as the corrosion products layer growth on the steel surface, the corrosion rate have shown a maximum value followed by a decrease at longer exposure times.

5. ACKNOWLEDGEMENTS

6. REFERENCES

[1] A. J. Bard, L. R. Faulkner, Electrochemical methods: Fundamentals and applications, Second ed., John Wiley & Sons, New York, 2001

[2] E. McCafferty, Introduction to corrosion science, First ed., Springer, New York, 2010

[3] L. L. Shreir, R. A. Jarman, G. T. Burnstein, Corrosion Vol. 1: Metal/Environmental reactions, Third ed., Butterworth Heinemann, Great Britain, 2000

[4] S. L. Chiu, J. R. Selman, J. Appl. Electrochem. 22 (1992) 28-37

[5] E. McCafferty, Corros. Sci. 47 (2005) 3202-3215

[6] B. W. A. Sherar, P. G. Keech, D. W. Shoesmith, Corros. Sci. 53 (2011) 3636-342

[7] L. Caceres, T. Vargas, M. Parra, Electrochem. Acta 54 (2009) 7435-7443

[8] W. Xing, G. Yin, J. Zhang, Rotating electrode methods and oxygen reduction electrocatalysts, First ed., Elsevier, Amsterdam, 2014

[9] A. Davydov, K. V. Rybalka, L. A. Beketaeva, G. R. Engelhardt, P. Jayaweera, D. D. Macdonald, Corros. Sci. 47 (2005) 195-215

[10] Y. Miyata, S. Asakura, Corros. Sci. 44 (2002) 589-602

[11] A. Soliz, L. Cáceres, J. Electrochem. Soc. 162 (8) (2015) C385-C395

[12] Y. Ma, Y. Li, F. Wang, Corros. Sci. 51 (2009) 997-1006

[13] K. Xiao, C. Dong, X. Li, F. Wang, J. Iron Steel Res. Int. 15 (5) (2008) 42-48

[14] T. Misawa, K. Hashimoto, S. Shimodaira, Corros. Sci. 14 (1974) 131-149

[15] M. Stratmann, J. Müller, Corros. Sci. 36 (1994) 327-359

[16] S. Zecevic, D. M. Drazic, S. Gojkovic, Corros. Sci. 32 (1991) 563-576